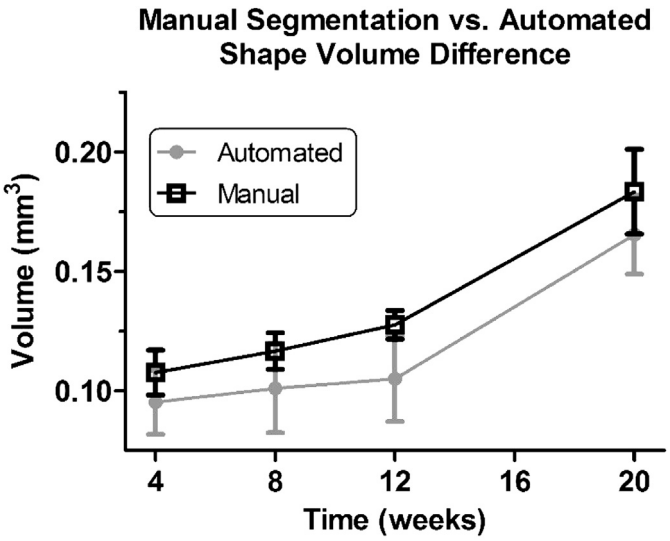

459
BONE MARROW LESIONS ARE SPATIALLY ASSOCIATED WITH DENUDED CARTILAGE IN OSTEOARTHRITIC KNEES: DATA FROM THE OSTEOARTHRITIS INITIATIVE

M.A. Bowes †, S.W. McLure ‡, C.B. Wolstenholme †, G.R. Vincent †, S. Williams ‡, P.G. Conaghan §. †*Imorphics Ltd, Manchester, United Kingdom;* ‡*Univ. of Leeds, Leeds, United Kingdom;* §*Leeds Inst. of Rheumatic and Musculoskeletal Med., Leeds, United Kingdom*

Purpose: Factors which affect the formation of bone marrow lesions (BML) in knee osteoarthritis (OA) are poorly understood. This study employed statistical shape modelling to study the spatial distribution of BMLs in all knee bones of an OA cohort, and compare this with the spatial distribution of denuded cartilage in the same knee joints.
Methods: A convenience cohort of 77 subjects with medial OA was identified from the NIH-OAI dataset. Subjects had K-L scores of 2 or 3; medial JSN > lateral JSN, medial osteophytes and ≥1° of varus malalignment. Baseline and 12 month images were segmented. BML were manually segmented in the TSE images, articular cartilage using the DESS images. Segmenters were blinded to time point but not to subject, using EndPoint software (Imorphics, UK). Bone surfaces were identified in both types of image by automated segmentation using active appearance models; this provides a reference bone surface in each image allowing for direct comparison of the BML and cartilage results. Cartilage thickness was measured on each cartilage plate using normal projection from the bone surface; thickness of less than 0.5 mm (the average size of 1 voxel edge) was considered as denuded. A semi-quantitative method for analysing the comparative position of the BML and denuded cartilage was developed. BML volumes were projected onto the bone surface, and the resultant area was displayed alongside the denuded cartilage from the same imaging visit. For each anatomical region if a BML was present it was scored as either overlapping the denuded area or not. 3-dimensional images of the characteristic BML spatial distributions were prepared by creating 3D surfaces of all BMLs, along with the bone surface in which they were found. These surfaces were linearly warped to the mean bone reference image, and a population image created which containing the number of BML 'hits' found at each voxel in the image. Typical' BML distribution was calculated by identifying all voxels in the reference image which had a value equal to or greater than half of the maximum number of recorded BMLs in any one voxel in the image.
Results: 38 of the subjects were women, mean age (SD) was 61.4 (9.9), and mean BMI was 30.9 (4.7). The majority of BML lesions were confined to 4 regions; 40 subjects had BML in the medial femorotibial region (MFT), 29 in the lateral patellofemoral region (LPF), 40 in the medial tibia (MT), and 25 in the lateral patella (LP). 72 subjects had BMLs present in more than one compartment. Mean volume of BML in each of these regions was MFT: 972 mm3, LPF: 954, LP: 745, MT: 1282. Overlap scoring for these 4 regions were as follows. MFT: 65%, MPF region: 87%, LPF: 69%, MT: 93%). Denuded cartilage showed a clear pattern in the femur and tibia, with denudation concentrated in regions rather than across the articulating surface. Denudation in the patella was more evenly distributed. 3D visualisation of the BML spatial distribution showed good agreement between the characteristic position of the BML volumes, and the areas of denuded cartilage (Fig. 1)
Conclusions: The study of BMLs is typically conducted using semi-quantitative methods, which do not provide good spatial information of either cartilage or BML lesions. The strong association between BML and denuded cartilage in this study is striking, and suggests that BMLs are at least in part caused by mechanical loading, which will be higher at regions lacking the protection of hyaline cartilage.

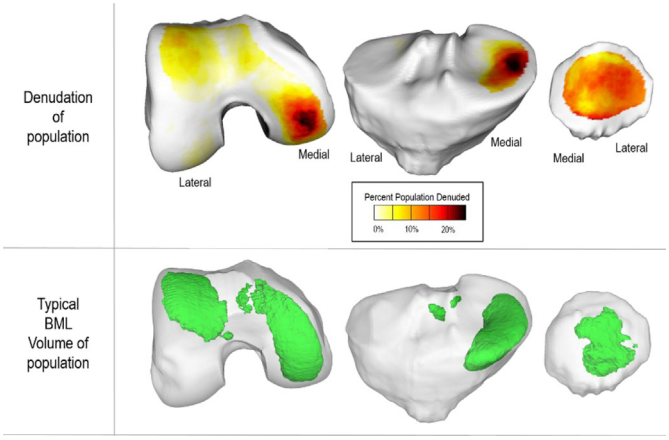

Fig. 1. Spatial comparison of summary population values for denuded cartilage (top row) with typical BML volume (bottom row) Denudation figures show the percentage of the population who have denuded cartilage at each point on the bone surface (scale in legend). BML volumes calculated as described in text.

460
BIOMECHANICAL KNEE CARTILAGE ANALYSIS IN YOUNG PROFESSIONAL SOCCER PLAYERS BY A T2 MAPPING UNLOADING ALGORITHM

G.H. Welsch, L. Waldenmeier, C. Evers, R. Janka, M. Uder, F. Hennig, M. Lochmann. *Univ. of Erlangen, Erlangen, Germany*

Purpose: High rates of knee osteoarthritis (OA) are known to occur in contact sports, with the highest rate in professional soccer players. The high demands to the knee joints may lead to repetitive trauma and possibly early cartilage injuries, nevertheless the an early onset in adolescence as well as possible correlating risk factors have not been studied so far using advanced imaging methodologies.
Aim of this study was to assess biomechanical loading and unloading parameters in the knee joints of adolescent professional soccer players by means of T2 Mapping analysis.
Methods: In this prospective study we analyzed the knee of the supporting leg of 60 healthy volunteers (17.1 ± 1.0years) of the junior section of a professional soccer team (all playing in the first national league in their respective junior team). Exclusion criteria were history of surgery or any traumatic knee lesion. Biochemical T2 mapping of the femoro-tibial joint was performed at 3-Tesla MRI using a zonal (superficial and deep) analysis (Fig. 1.) T2 mapping was performed immediately after loading and 30 minutes after unloading (Fig. 2.) Region-of-Interest analysis was performed by two observers followed by statistical Analysis-of-Variance to assess differences in between loaded and unloaded cartilage with respect to the different anatomical zones (Fig. 1). Additionally clinical scores and knee function analyses were assessed.
Results: The reproducibility was very high in all knee compartments (ICC > 0.9). T2 values (ms) showed to be different in between the anatomical zones, most obvious in between the femoral condyles and the tibial cartilage ($p < 0.05$). When comparing loading to unloading, a clearly significant increase of the T2 values was present in the superficial cartilage zones of the anterior (loading: 52.8 ± 10.6 ms; unloading: 55.3 ± 11.6 ms; $p = 0.016$) and central (loading: 63.8 ± 11.9 ms; unloading: 67.1 ± 12.9 ms; $p = 0.005$) femoral condyle. The underlying deep cartilage zone (anterior (loading: 38.6 ± 11.4 ms; unloading: 39.9

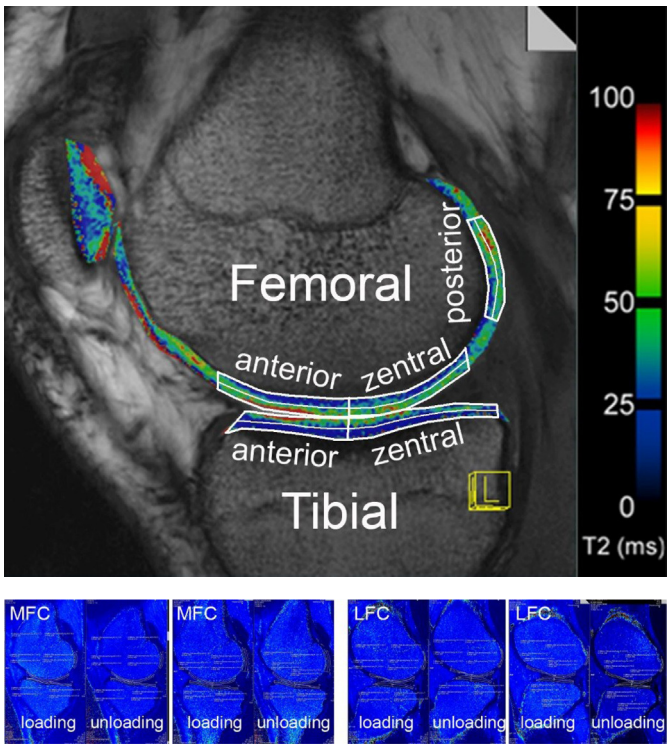

± 11.7 ms; p = 0.217) and central (loading: 43.4 ± 10.0 ms; unloading: 44.6 ± 11.0 ms; p = 0.214)) of the weight-bearing aspect of the femoral condyle, as well as all other cartilage areas (Tibial anterior (sup./deep): loading: 43.2 ± 8.8/30.8 ± 7.3 ms, unloading: 44.2 ± 9.8/31.1 ± 6.9; p = 0.276 and 0.678); (Tibial central (sup./deep): loading: 47.2 ± 8.5/31.1 ± 6.3, unloading: 47.8 ± 10.0/31.3 ± 7.1; p = 0.463 and 0.693); (as well as femoral posterior (sup./deep): loading: 58.8 ± 13.1/46.6 ± 10.1, unloading: 58.3 ± 12.7/45.3 ± 9.2; p = 0.695 and 0.144) did not reveal a significant difference of the T2 values.

Conclusions: This prospective analysis is the first available approach to understand cartilage kinematics in young professional soccer players and to prevent cartilage injuries. The increase of the T2-values during unloading takes place in the area were traumatic and osteochondral cartilage lesions usually appear and were most often osteoarthritic changes take place in later years. The presented approach may help to monitor soccer players at high risk for cartilage injuries.

461
QUANTITATIVE MRI (QMRI) FEATURES PREDICT SYMPTOMATIC KNEE PAIN DURING THE NEXT YEAR: DATA FROM THE OAI

J.G. Tamez-Pena †, J. Farber ‡, J.I. Galvan-Tejada †, E. Schreyer ‡, V. Treviño †, P.C. Gonzalez ‡, S. Totterman ‡. † *ITESM, Monterrey, Nuevo Leon, Mexico;* ‡ *Qmetrics Technologies, Rochester, NY, USA*

Purpose: Predicting those who will develop near-term chronic knee pain may accelerate the development of effective OA therapies. The purpose of this work was: 1) To describe the qMRI differences between subjects with and without symptomatic knee pain; 2) To develop a 12-month predictive index of symptomatic knee pain based on qMRI analysis.

Methods: Subjects from the Osteoarthritis Initiative (OAI) with untreated right knee pain were selected for this study. Those whose right knee symptomatic pain scores (RKSX) were 2, indicating "Pain most days of a month in past 12m" and whose corresponding RKSX scores for the prior year were lower were included. Age, BMI and gender matched subjects without right knee pain were selected as a control cohort. 3D DESS WE MRI images were analyzed using software (Qmetrics Technologies, Rochester, NY) that automatically segmented articular cartilage into whole femur, tibia and patella, and sub-regional central medial femur, central lateral femur, medial tibia, lateral tibia, medial trochlea, lateral trochlea, medial patella, and lateral patella. A human observed qualified the success of the segmentations. Segmentations that failed to accurately delineate cartilage tissue were removed from the analysis. Cartilage volume, area, thickness, curvature and DESS signal contrast properties were computed for each region. Descriptive statistics were generated for thickness, curvature and signal contrast measurements. All measurements were adjusted for BMI, age and gender differences. Next, the measurements were z-transformed using the rank inverse normal transform. Finally, individual measurements were classified as low-control-quartile ($p < 0.25$), mid-control-range ($0.25 < p < 0.75$) and top-control-quartile ($p > 0.75$). At each class the z-score was maintained. The qMRI analyses at the time of recording the RKSX = 2 observation (T-0) and year prior (T-1) were selected. Matching T-0 visit was determined for the control group, based on the T-0 visit of the age-gender-BMI matched case subject. Multivariate logistic models were used to build a Knee-pain predictor. The model selection was found using a bootstrapped-step-wise feature selection algorithm based on the Integrated Discrimination Improvement (IDI). Knee-pain-models were developed for the T-1 and T-0 time points, and both models were internally validated using a tenfold cross-validation. The odds ratio (OR) for each model feature was evaluated. Finally, we determine the practicality of the index to select patients that will develop pain in the next by determining of the number of subjects that could be correctly predicted with a 5% false positive rate.

Results: At pain incidence (RKSX = 2), 77 cases with reliable qMRI analyses were included (38:39 Males:Females). 165 controls were matched at the incident point (84:81 Males:Females). The entire cohort had an average age of 66.21 ± 9.5 years with a BMI of 26.9 ± 4.6. Subjects with available prior year qMRI analyses included 60 cases and 138 controls. Table 1 shows the qMRI parameters that were able to separate cases from controls at the time of pain incidence and one year prior. The model at pain incidence indicated that superficial femur signal contrast, the curvature of the tibia, and patella were different between cases and controls with odds ratios of 3.38, 4.5 and 4.15 respectively. One year prior to the incidence of pain, the thickness of patella cartilage, the cartilage signal contrast of the medial patella and that of the femur were discriminant between subjects that progressed to pain and subjects that did not. The odds were 11.0, 3.0 and 1.8 respectively. The model at one year prior to pain onset was able to accurately predict 28% of the subjects that progress to pain with only 5% false positives.

Table 1
qMRI features that separate subjects without pain from subjects with symptomatic knee pain.(−) OR for differences al the low-control-quartile. (+) OR for differences in the lop-control-quartile.

Model	Description	Cases	Control	Odds Ratio
T-0 AUC 0.80 (0.73–0.87), Sensitivity 36% at 95% Specificity	Femur Contrast (Mean)	2.131 (0.608)	2.485 (0.562)	3.38 (2.20-5.18) (−)
	Medial Paid la Area	418.5 (63.7)	434.8 (85.7)	6.21 (1.62–23.77)
	Tibia Curvature (Trimmed)	−0.012 (0.006)	−0.009 (0.006)	4.54 (1.28–16.14)
	Tibia Area	1855.1 (247.1)	1930.5 (310.2)	7.20 (1.86–27.83)
	Patella Curvature (Mean)	0.009 (0.008)	0.011 (0.006)	4.15 (1.23–14.02)
	Lateral Trochlea Contrast (5%)	−2.453 (1.551)	−2.702 (1.612)	1.94 (1.16–3.23) (+)
	Lateral Tibia Contrast (95%)	3.663 (0.877)	3.991 (0.852)	3.75 (1.07–13.15)
T–1 AUC on (0.75–0.88) Sensitivity 0.28 at 0.95 Sensitivity)	Patella Thickness (5%)	0.708 (0.037)	0.714 (0.037)	11.01 (2.38–50.93)
	Medial Patella Contrast (Std)	1.376 (0.294)	1.301 (0.222)	3.02 (1.73–5.29) (+)
	Femur Contrast (Mean)	2.131 (0.608)	2.485 (0.562)	1.80 (1.06–3.06) (−)
	Patella Contrast (Std)	1.777 (0.478)	2.000 (0.439)	2.15 (1.24–3.70) (−)
	Lateral Patella Curvature (Std)	0.059 (0.005)	0.060 (0.007)	2.65 (1.37–5.14) (−)
	Lateral Trochlea Thickness (Std)	0.678 (0.131)	0.668 (0.138)	0.11 (0.03–0.52)